Synthesis of an Efficient Pb Adsorption Nano-Crystal under Strong Alkali Hydrothermal Environment Using a Gemini Surfactant as Directing Agent

[1]Chen Chen*, [2]Ting Cheng, [3]Xiao Zhang, [2]Ruixin Wu and [2]Qingying Wang
[1]School of Environmental and Chemical Engineering, Jiangsu University of Science and Technology, Zhenjiang 212005, China.
[2]Department of City Science, Jiangsu City Vocational College, Nanjing 210036, China.
[3]Nanjing University and Yancheng Academy of Environmental Technology and Engineering, Yancheng 224000, China.
chenc@just.edu.cn*

(Received on 25th January 2018, accepted in revised form 7th March 2019)

Summary: Using a gemini surfactant ($[C_{18}H_{37}(CH_3)^2\text{-}N^+\text{-}(CH_2)_3\text{-}N^+\text{-}(CH_3)_2C_{18}H_{37}]Cl_2$) as the directing agent, K_2SiO_3 and $KAlO_2$ as the source of silicon and aluminum, a Nano-crystal has been successfully synthesized under a strong alkali hydrothermal condition. The material shows hexahedron morphology and its crystal size is between around 250-500 nm. Its liquid specific surface area is 1313.2 $m^2 \cdot g^{-1}$. The adsorption process of Pb on the Nano-crystal follows quasi-second-order kinetic model and Langmuir adsorption isotherm equation. The maximum Pb adsorption capacity of Nano-crystal is around 1105 $mg \cdot g^{-1}$.

Keywords: Nanoparticles; Nanocrystalline materials; Crystal growth; Gemini surfactant; Adsorption; Pb.

Introduction

Pb is much harmful to both the environment and human's health [1-3]. According to the standard of China Ministry of environmental protection, the concentration of Pb in waste water must be lower than 1.0$mg \cdot L^{-1}$. At present, absorption process is one of the effective, convenient and rapid methods to remove Pb from waste water [4-6]. Now, an efficient Pb adsorption Nano-crystal has been successfully synthesized under an alkali hydrothermal environment and using a gemini surfactant ($[C_{18}H_{37}(CH_3)^2\text{-}N^+\text{-}(CH_2)_3\text{-}N^+\text{-}(CH_3)_2C_{18}H_{37}]Cl_2$) as directing agent. After successfully synthesized, the adsorption capacity of Nano-crystal is proved by Pb adsorption environment.

Experimental

Potassium silicate (Analytically pure), potassium hydroxide (Analytically pure) and lead nitrate (Analytically pure) used in the experiment were purchased from China national pharmaceutical chemical reagent Co. Ltd. Partial potassium aluminate (Chemical purity) was purchased from Shandong Luke chemical industry Co. Ltd, China. $[C_{18}H_{37}(CH_3)^2\text{-}N^+\text{-}(CH_2)_3\text{-}N^+\text{-}(CH_3)_2C_{18}H_{37}]Cl_2$ (98%) were purchased from Henan Daochun Chemical Technology Co., Ltd, China. The synthesis system of Nano-crystal was as follow: 6.1087g potassium silicate, 2.744g partial potassium aluminate and 0.1819g directing agent were added into a teflon bottle which contains potassium hydroxide (240ml, 10$mol \cdot L^{-1}$) solution. A water bath reaction device installed on a magnetic stirrer keep the reaction temperature around 348K (±2K). During the synthesis process, magnetic stirrer maintained stirring the reaction systems and the reaction time was 10 hours. After synthesis finished, deionized water was used to wash the reaction products until the pH value of filter liquor is around 7. Ultimately, reaction product was dried fewer than 383K and the final product is Nano-crystal.

Material characterization methods used in this experiment was X-ray diffraction analysis which is from Thermo's type X 'TRA X-ray diffractometer. The morphology and microscopic composition of the Nano-crystal were analyzed by using the scanning electron microscope of HITACHI (S-3400N). Liquid specific surface area was measured by liquid specific surface area analyzer of Xigo company. The adsorption experiment is a typical static adsorption experiment. The range of pH value in adsorption system is from 2-9. The range of adsorption temperature is from 308 to 348K. The range of absorption time is from 15 to 480min. The range of Pb concentration is 300-1750mg/L. The concentration of Pb is measured by atomic absorption spectrophotometer (Agilent, AA240DUO).

*To whom all correspondence should be addressed.

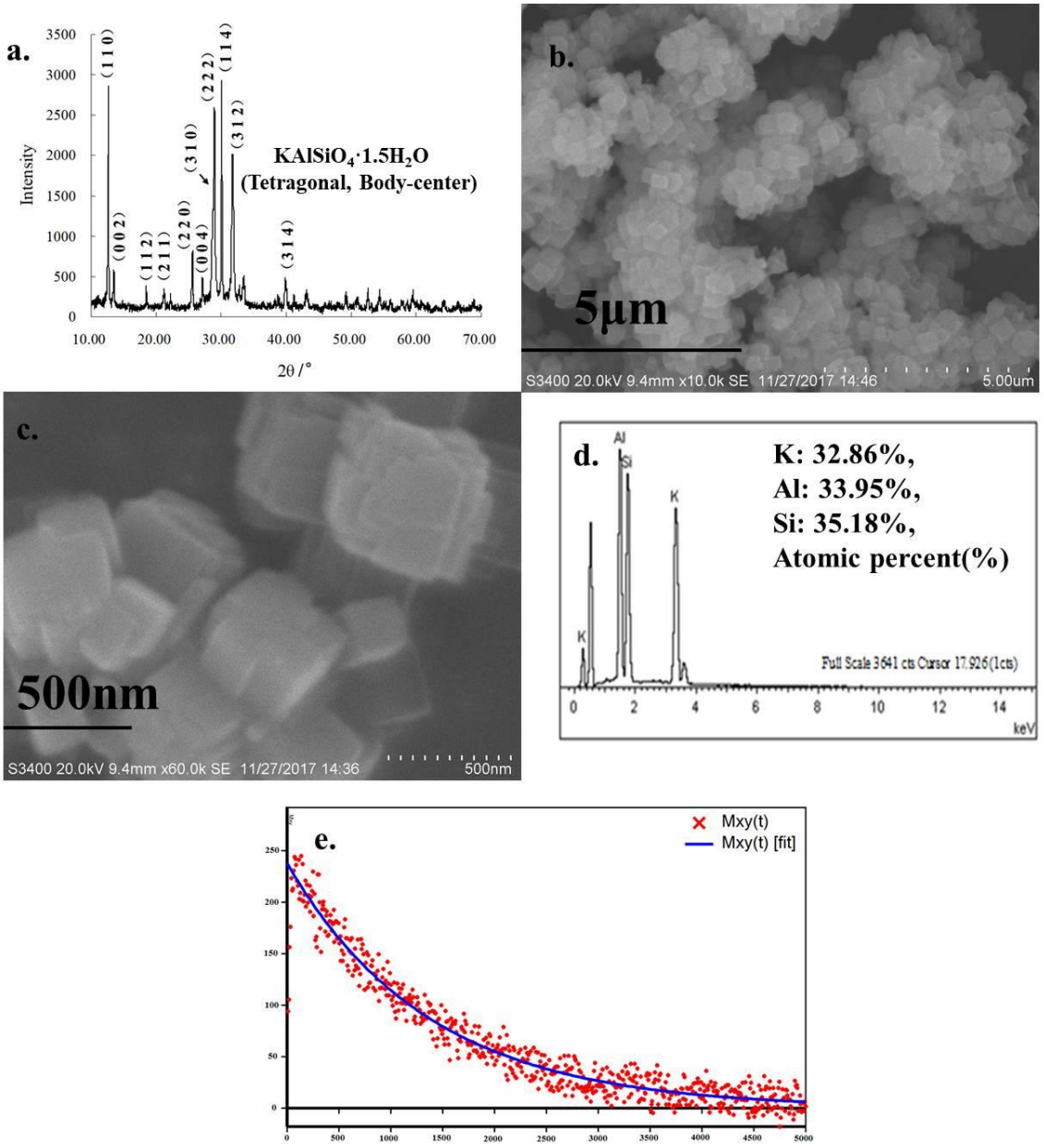

Fig1. (a) XRD pattern, (b) and (c) SEM, (d) EDX, (e) liquid specific surface area of Nano crystal.

Results and Discussions

Fig1.a demonstrates the XRD pattern of Nano-crystal. From Fig. 1a, it could be seen that the main XRD peak of Nano-crystal appears at 2θ (28.981°), (28.681°), (31.701°), (30.081°), (12.682°) and (13.481°) should belong to $KAlSiO_4 \cdot 1.5H_2O$ (Tetragonal, Body-center, PDF-No. 38-0216). Fig. 1b and Fig. 1c show the SEM of Nano-crystal. The Nano-crystal shows hexahedron morphology, which is consistent with XRD result. The crystal size is around 250-500nm. The gain of this Nano-scale microstructure is mainly attributed to the restriction function of the directing agent $[C_{18}H_{37}(CH_3)^2\text{-}N^+\text{-}(CH_2)_3\text{-}N^+\text{-}(CH_3)_2C_{18}H_{37}]Cl_2$ [7-9]. Compared with the previous related research of microcrystal, the XRD results of the Nano-crystal showed a significant decrease in the intensity of main diffraction peak at (110), (310) and (312), which indicated the growth of (110), (310), (312) planes were inhibited during the synthesis process of Nano-crystals. Moreover, this result illustrated the

inhibition of certain specific planes growing during the crystal growth by the addition of gemini surfactant [10]. Fig1.e shows the EDX analysis result of a 1200μm×900μm area and the main composition of Nano-crystal is K, Al, Si. The molar ratio of element is K: 32%, Al: 33%, Si: 35%, which is consistent with its molecular formula ($KAlSiO_4 \cdot 1.5H_2O$). The liquid specific surface area of Nano-crystal is 1313.2 $m^2 \cdot g^{-1}$ (Fig1.f).

The adsorption kinetics model and adsorption isotherm model are as follow:

The Lagergren pseudo-first-order model [11, 12]

$$Ln(Q_e - Q_t) = LnQ_e - k_1 t \quad (1)$$

where Q_e ($mg \cdot g^{-1}$) is equilibrium adsorption capacity of Pb on Nano-crystal, Q_t ($mg \cdot g^{-1}$) is adsorption capacity of Pb on Nano-caystal at time t, k_1 (min^{-1}) is rate constant of first-order model and t (min) is contact time.

The Blanchard pseudo-second-order model [13, 14]

$$\frac{t}{Q_t} = \frac{1}{k_2 Q_e^{\,2}} + \frac{t}{Q_e} \quad (2)$$

where k_2 ($g \cdot mg^{-1} \cdot min^{-1}$) is rate constant of second-order model.

The equation of Langmuir isotherm [15, 16] is as follow:

$$\frac{C_e}{Q_e} = \frac{1}{k_L Q_m} + \frac{C_e}{Q_m} \quad (3)$$

where Q_e ($mg \cdot g^{-1}$) and C_e ($mg \cdot L^{-1}$) are the amount Pb adsorbed and the Pb concentration on solution, both at equilibrium; k_L ($L \cdot mg^{-1}$) is the Langmuir constant related to the energy of adsorption; and Q_m ($mg \cdot g^{-1}$) is the maximum adsorption capacity.

The equation of Freundlich isotherm [17] is as follow:

$$\mathrm{Ln}(Q_e) = \mathrm{Ln}(k_F) + \frac{1}{n}\mathrm{Ln}(C_e) \quad (4)$$

where k_F and n are constants for the Freundlich isotherm, they are indicative of the adsorption capacity ($mg \cdot g^{-1}$) and adsorption intensity.

Fig2.a shows the effects of adsorption temperature and time on the adsorption capacity, from which we can see that the higher temperature will lead to the decrease of adsorption capacity. The adsorption kinetics and isotherm of Pb by Nano-crystal was analyzed and the results are shown in Fig2.b, Fig2.c and Table1. It could be seen that the adsorption process of Pb by Nano-crystal is better accord with the quasi-second-order kinetic model and the R^2 is higher than 0.997. The Langmuir adsorption isotherm model can be used to fit the adsorption process of Pb ions on Nano-crystal and the R^2 is 0.9998. The maximum Pb adsorption capacity is 1105 $mg \cdot g^{-1}$. The adsorption capacity is higher than novel porous tablet material (215.52 $mg \cdot g^{-1}$)[18], microwave-assisted functionalized lignin (106$mg \cdot g^{-1}$) [1], modified magnetic nanoparticles (333.3$mg \cdot g^{-1}$)[5], porous biosilica (120.4$mg \cdot g^{-1}$)[19], modified chitosan/$CoFe_2O_4$ particles(228.3$mg \cdot g^{-1}$)[13] and is similar with Cu/ZnO composite (1111 $mg \cdot g^{-1}$)[4]. Fig2.d indicates the effect of solution pH on adsorption capacity. It could be seen that the adsorption capacity would increase with rise of solution pH.

Table-1: Adsorption process parameters of Pb on Nano-crystal.

Adsorption kinetics				
Quasi-first-order				
Temperature (K)	**k_1(min^{-1})**	**Q_{cal}($mg.g^{-1}$)**	**Q_{exp}($mg.g^{-1}$)**	**R^2**
308	**0.01463±0.00603**	**441.02±4.25**	**996±18.6**	**0.972**
323	**0.01097±0.00598**	**539.69±4.14**	**760±18.7**	**0.933**
348	**0.00913±0.00565**	**484±3.85**	**531±16.6**	**0.983**
Quasi-second-order				
Temperature (K)	**k_2 ($g.mg^{-1}.min^{-1}$)**	**Q_{cal}($mg.g^{-1}$)**	**Q_{exp}($mg.g^{-1}$)**	**R^2**
308	**0.00009276±0.000004787**	**1005.13±7.63**	**996±18.6**	**0.995**
323	**0.00005523±0.000002548**	**775.19±8.32**	**760±18.7**	**0.986**
348	**0.00002448±0.000001419**	**606.06±10.89**	**531±16.6**	**0.992**
Adsorption isotherm				
Langmuir isotherm				
k_L($L.mg^{-1}$)		**Q_m($mg.g^{-1}$)**		**R^2**
0.1091±0.0042		**1084.48±10.94**		**0.986**
Freundlich isotherm				
k_F		**n**		**R^2**
289.31±9.96		**4.29±10.153**		**0.871**

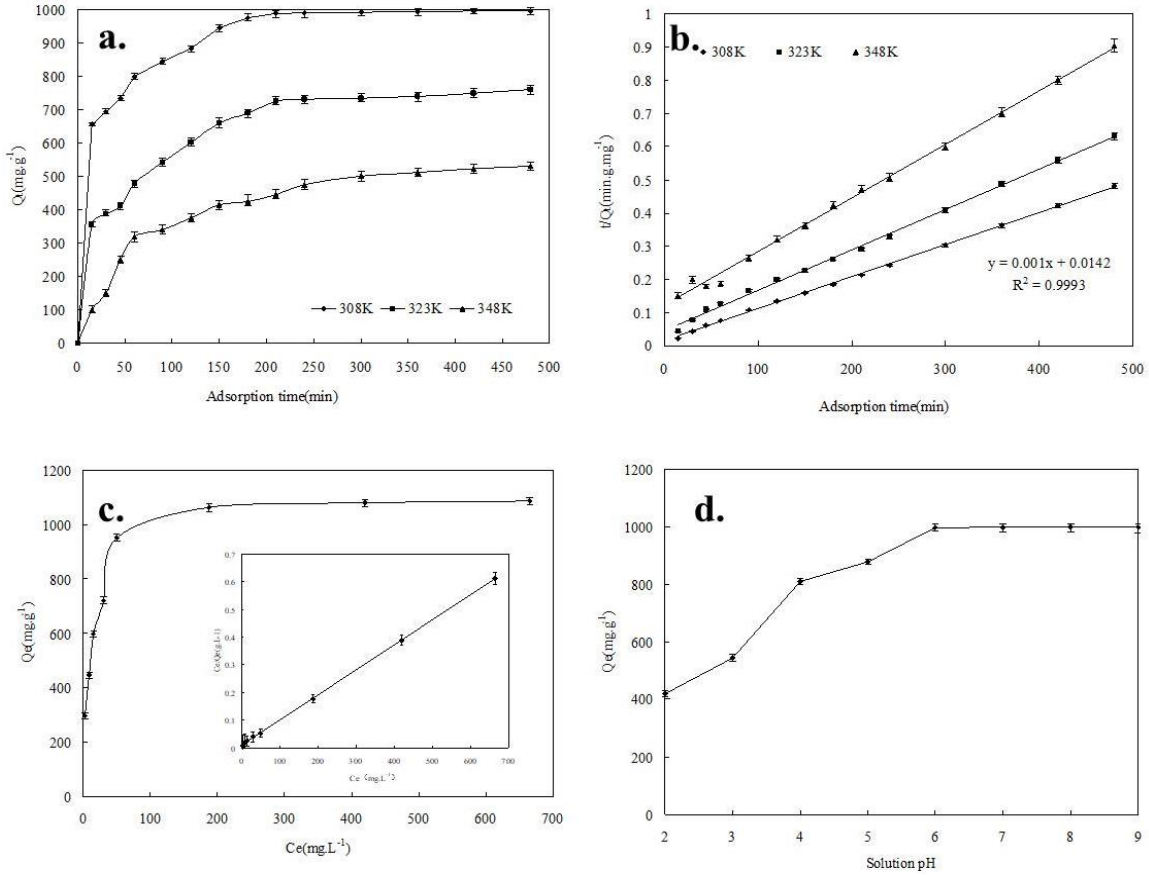

Fig 2: (a) Effect of time and temperature on adsorption capacity, (b) Quasi-second-order kinetics model fitting result, (c) The relationship between equilibrium concentration and adsorption capacity (insert, Langmuir isotherm model fitting result), (d) Effect of solution pH on adsorption capacity.

Conclusions

Using $[C_{18}H_{37}(CH_3)^2\text{-}N^+\text{-}(CH_2)_3\text{-}N^+\text{-}(CH_3)_2C_{18}H_{37}]Cl_2$ as directing agent, potassium silicate and partial potassium aluminate as the source of silicon and aluminum source, the Nano-crystal has been successfully synthesized under the alkali hydrothermal conditions. The morphology of this material shows hexahedron and its crystal size is between around 250-500 nm. Its liquid specific surface area is $1313.2 m^2 \cdot g^{-1}$. The adsorption process of Pb on the Nano-crystal is in accord with quasi-second-order kinetic model and Langmuir adsorption isotherm equation. Nano-crystal has a maximum Pb adsorption capacity of 1105 $mg \cdot g^{-1}$.

Acknowledgment

This work was financial supported by the Natural Science Foundation of China (Grant No. 21407068), 2016 University of Jiangsu Province Blue Project of young academic leader training objects, Jiangsu Science and Technology Program - a prospective joint research project (Grant No. BY2016068-01), Science Foundation of Jiangsu Colleges and Universities (Grant No. 17KJD610001, 17KJD610002).

Reference

1. M. Yan, Z. Li, Microwave-assisted functionalized lignin with dithiocarbamate for enhancing adsorption of Pb(II), *Mater. Lett.*, **170**, 135 (2016).
2. S. Deng, P. Wang, G. Zhang, Y. Dou, Polyacrylonitrile-based fiber modified with thiosemicarbazide bymicrowave irradiation and its adsorption behavior for Cd(II) and Pb(II), *J. Hazard. Mater*., **307**, 64 (2016).
3. D.L. Hughes, A. Afsar, L.M. Harwood, T. Jiang, D.M. Laventine, L.J. Shaw, M.E. Hodson,

Adsorption of Pb and Zn from binary metal solutions and in the presence of dissolved organic carbon by DTPA-functionalised, silicacoated magnetic nanoparticles, *Chemosphere*., **183**, 519 (2017).

4. A. Modwi, L. Khezami, Kamal Taha, O.K. Al-Duaij, Ammar Houas, Fast and high efficiency adsorption of Pb(II) ions by Cu/ZnO composite, *Mater. Lett.*, **195**, 41 (2017) .
5. S.F. Jiryaei, A. Shahbazi, Melamine-based dendrimer amine-modified magnetic nanoparticles as an efficient Pb(II) adsorbent for wastewater treatment: Adsorption optimization by response surface methodology, *Chemosphere.*, **189**, 291 (2017).
6. C. Zhang, Z. Yu, G. Zeng, B. Huang, H. Dong, J. Huang, Z. Yang, J. Wei, L. Hu, Q. Zhang, Phase transformation of crystalline iron oxides and their adsorption abilities for Pb and Cd, *Chem. Eng. J*., **284**, 247 (2016).
7. K. Na, C. Jo, J. Kim, K. Cho, J. Jung, Y. Seo, R.J. Messinger, B.F. Chmelka, R. Ryoo, Directing zeolite structures into hierarchically nanoporous architectures, *Science*., **333**, 328(2011).
8. S.W. Han, J. Kim, R. Ryoo, Dry-gel synthesis of mesoporous MFI zeolite nanosponges using a structure-directing surfactant, *Microporous Mesoporous Mat*., **240**, 123 (2017).
9. M. Choi, K. Na, J. Kim, Y. Sakamoto, O. Terasaki, R. Ryoo, Stable single-unit-cell nanosheets of zeolite MFI as active and long-lived catalysts, *Nature*., **461**, 246 (2009).
10. M.S. Bakshi, P. Thakur, S. Sachar, G. Kaur, Aqueous Phase Surfactant Selective Shape Controlled Synthesis of Lead Sulfide Nanocrystals, *J. Phys. Chem. C*., **111**, 18087 (2007).
11. K. B. Tan, A. Z. Abdullah, B. A. Horri, B. Salamatinia, Adsorption mechanism of microcrystalline cellulose as green adsorbent for the removal of cationic methylene blue dye, *J.Chem.Soc.Pak.*, **38**, 651 (2016).
12. H. Zhang, L. Gu, L. Zhang, S. Zheng, H. Wan, J. Sun, D. Zhu, Z. Xu, Removal of aqueous Pb(II) by adsorption on Al_2O_3-pillared layered MnO_2, *Appl. Surf. Sci.*, **406**, 330 (2017).
13. C. Fan, K. Li, J. Li, D. Ying, Y. Wang, J. Jia, Comparative and competitive adsorption of Pb(II) and Cu(II) using tetraethylenepentamine modified chitosan/$CoFe_2O_4$ particles, *J. Hazard. Mater.*, **326**, 211(2017).
14. Q. Xu, Y. Wang, L. Jin, Y. Wang, M. Qin, Adsorption of Cu (II), Pb (II) and Cr (VI) from aqueous solutions usingblack wattle tannin-immobilized nanocellulose, *J. Hazard. Mater*. **339**, 91(2017).
15. Y. Zhang, J. Yang, B. Liu, Y. Xu, Removal of copper ions from water using chemical modified multi-walled carbon nanotubes, *J.Chem.Soc.Pak.*, **36**, 841 (2014).
16. A. Abbas, R. Rehman, S. Murtaza, U. Shafique, Adsorptive removal of congo red and sunset yellow dyes from water systems by lady finger stem, *J.Chem.Soc.Pak.*, **34**, 1241 (2012).
17. F. Kanwal, R. Rehman, J. Anwar, M. Saeed, Batchwise removal of Chromium (VI) by adsorption on novel synthesized polyaniline composites with various brans and isothermal modeling of equilibrium data, *J.Chem.Soc.Pak.*, **34**, 1134 (2012)
18. H. Ma, Y. Hei, T. Wei, H. Li, Three-dimensional interconnected porous tablet ceramic: Synthesis and Pb(II) adsorption, *Mater. Lett.*, **196**, 396 (2017).
19. Y. Qi, J. Wang, X. Wang, J.J. Cheng, Z. Wen, Selective adsorption of Pb(II) from aqueous solution using porous biosilica extracted from marine diatom biomass: Properties and mechanism, *Appl. Surf. Sci*., **396**, 965 (2017).